# EFFECTS OF NEUROPEPTIDE-Y (NPY) ON BONE METABOLISM AS A NEUROMEDIATOR

A THESIS SUBMITTED TO

THE GRADUATE SCHOOL OF NATURAL AND APPLIED SCIENCES

OF

THE MIDDLE EAST TECHNICAL UNIVERSITY

BY

MUAMMER ÖZGÜR ÇEVİK

IN PARTIAL FULFILLMENT OF THE REQUIREMENTS FOR THE DEGREE OF
MASTER OF SCIENCE
IN
THE DEPARTMENT OF BIOTECHNOLOGY

MARCH 2004

Approval of the Graduate School of Natural and Applied Sciences

Prof. Dr. Canan ÖZGEN
Director

I certify that this thesis satisfies all the requirements as a thesis for the degree of Master of Science.

Associate Prof. Dr. F. Dilek SANİN
Head of Department

This is to certify that we have read this thesis and in our opinion it is fully adequate, in scope and quality, as a thesis for the degree of Master of Science.

Dr. Alpaslan ŞENKÖYLÜ
Co-supervisor

Prof. Dr. Feza KORKUSUZ
Supervisor

Examining Committee Members

Prof. Dr. M. Ruşen GEÇİT

Prof. Dr. Aykut ÖZKUL

Prof. Dr. Feza KORKUSUZ

Associate Prof. Dr. Serhat AKIN

Associate Prof. Dr. Hasan BİLGİLİ

## ABSTRACT

## EFFECTS OF NEUROPEPTIDE Y (NPY) ON BONE METABOLISM AS A NEUROMEDIATOR



**ÇEVİK, M. Özgür**

**M. Sc., Department of Biotechnology**

**Supervisor: Prof. Dr. Feza KORKUSUZ**

**Co-Supervisor: Dr. Alpaslan ŞENKÖYLÜ**



**March 2004, 71 pages**



Periosteum of bone is highly innervated and evidence for a regulation of bone metabolism by nerve fibers has been suggested by many clinical and experimental studies. However the nature of the neuromediators involved in these processes has not been well documented. Neuropeptide –Y (NPY) is a neuromediator which is found to have receptors through the bone tissue and among these neuromediators its actions remains to be elucidated.

In order to elucidate the effects of NPY directly on bone tissue, two different doses of NPY (NPY dose 1= $1X10^{-5}$ M and NPY dose 2 = $1X\ 10^{-6}$ M) and NPY dose 2 plus its inhibitor were applied together with hyaluronic acid (HA) into the intramedullary area of right tibia of Wistar rats. HA alone was administered as the control group. On three time points, day one, week one and week two after administration, the tibiae were collected and stored at –20°C for analysis.

Evaluation was performed via conventional radiography, dual energy X-ray absorbtiometry (DEXA), quantitative computerized tomography (QCT), three point bending test (TPB) and histology techniques. QCT was used to assess both atomic content and density of both medulla and cortex of tibiae.

From DEXA results, it was observed that inhibition of NPY causes an increase in the bone mass from first day to second week. This phenomena was also observed in histology results so that new bone formation in the inhibitor administered bone was encountered at week two. In both medulla and cortex areas' atomic content, an increase in average effective atomic number was displayed after administration of NPY plus NPY inhibitor throughout two weeks. In addition, density of medulla of tibiae measured by QCT also revealed an increase in bone mass when inhibitor is applied throughout two weeks.

As a result, overall evaluation of data obtained from DEXA, QCT and histological analysis revealed that NPY inhibits bone formation or have a pro-osteoclastic effect; inversely HA displayed osteogenic effect .

Keywords: Neuropeptide-Y, bone, three point bending, DEXA, computerized tomography, density, atomic content, neuromediators,

# ÖZ

## NÖROPEPTİD-Y' NİN NÖROMEDİYATOR OLARAK KEMİK DOKUSUNA ETKİLERİ

**ÇEVİK, M. Özgür**
**Yüksek Lisans, Biyoteknoloji Bölümü**
**Tez Yöneticisi: Prof. Dr. Feza KORKUSUZ**
**Ortak Tez Yöneticisi: Dr. Alpaslan ŞENKÖYLÜ**

**Mart 2004, 71 sayfa**

Kemik dokusunun periostunun yoğun olarak sinir ağıyla çevrelendiği ve sinir sisteminin kemik metabolizmasının düzenlenmesinde etkin rol aldığı birçok klinik ve deneysel çalışma tarafından ortaya konmuştur. Ancak bu süreçte rol alan nöromediyatörlerin etkileri henüz tam olarak açıklığa kavuşmamıştır. Kemik dokusuna etki eden nöromediyatörlerden olan ve kemik dokusunda reseptörlerine rastlanan nöropeptid-Y (NPY)'nin de kemik dokusundaki etkileri henüz tanımlanamamıştır.

NPY'nin kemik dokusundaki etkilerini araştırmak için NPY'nin iki farklı dozu (NPY doz 1=1X10$^{-5}$ M ve NPY doz 2=1X10$^{-6}$ M), NPY doz 2 artı NPY inhibitörü hyaluronik asit (HA) eşliğinde Wistar cinsi sıçanların

sağ tibialarının intramedüllerine uygulanmıştır. Hyalüronik asit ise tek başına kontrol grubu olarak uygulanmıştır Sıçanların tibiaları uygulamadan sonraki birinci günde, birinci haftada ve ikinci haftada alınıp, -20° C' de sonraki analizler için saklanmıştır.

Bu çalışmada radyografi, kemik dansitometresi (DEXA), kantitatif bilgisayarlı tomografi (QCT), üç nokta kırılma testi ve histolojik metodlar kullanılmıştır. Bilgisayarlı tomografi, tibia örneklerinin hem atomik içeriğini hem de kemik yoğunluğunu kortikal ve medüller olarak ölçmek için kullanılmıştır.

DEXA sonuçlarına göre NPY'nin inhibisyonu birinci günden ikinci haftaya kadar kemik yoğunluğunda artışa sebep olmuştur. Buna benzer bir sonuç histolojik analizlerde, inhibitör ve NPY'nin birlikte uygulandığı tibiada, ikinci haftada, kemik oluşumu olarak gözlemlenmiştir. İki hafta süresince, hem medullanın hem de korteksin atomik içeriklerinin ortalaması, NPY ve inhibitörün birlikte uygulanmasıyla zamana bağlı artış göstermiştir. Buna ek olarak, NPY ve inhibitör birlikte uygulandığında, QCT ile ölçülen kemik yoğunluğunda tibiaların medüller yoğunluğunun iki hafta süresince ortalama olarak arttığı gözlemlenmiştir.

Sonuçta, DEXA, QCT ve histolojik ölçümlerin ışığında NPY'nin kemik oluşumunu inhibe ettiği ya da pro-osteoclastik etkisinin bulunduğu saptanmıştır. Aksine, literatürle de uyumlu olarak HA'nın kemik yapımına yol açtığı saptanmıştır.

Anahtar Kelimeler: Nöropeptid-Y, kemik , üç nokta kırılma testi, DEXA, kantitatif bilgisayarlı tomografi, atomik içerik, nöromediyatörler.

**To the young scientists of Turkey and their families who are dedicated to the improvement of Turkish science despite all difficulties.....**

## ACKNOWLEDGEMENT

I would like to express my sincerest gratitude to my supervisor Prof. Dr. Feza KORKUSUZ who encouraged and supported me to find my way as a scientist candidate. I will always take him as a model in his humanity, discipline, passion and dedication to development of our country.

I would like to express my deepest respect and thanks to my co-supervisor Dr. Alpaslan ŞENKÖYLÜ who patiently solved my problems of all kind like a young father. He donated his valuable grant to me to obtain rats for the experiments and donate his valuable weekends for operations with me rather than spending with his little daughter.

I am delighted to thank to Prof. Dr. M. Ruşen GEÇİT and his assistants Arzu Gül TAŞÇI and Dr. Mehmet YETMEZ for enhancing three point bending test.

I would like to thank to Prof. Dr. Aykut ÖZKUL for preparing my gels and solutions for many times and helping in obtaining and storing the chemicals that we used.

I am very grateful to Associate Professor Serhat AKIN and his assistant Ömer İZGEÇ for their invaluable patience in capturing and image analysis of QCT data. I am sorry and full of respect for yours sleepless nights.

I am also grateful to Assoc. Prof. Petek KORKUSUZ who both dealt with my samples' histologic analysis and with a very energetic, pretty boy ATA at the same time. I hope mine was not as tiring as the second one.

I would like to thank to Assoc. Prof. Kamil Can AKÇALI from Bilkent University Department of Molecular Biology and Genetics for helping me to find rats for my experiments.

I would like to thank to physcologist Sedat IŞIKLI for his help in statistical analysis and counseling.

Last of all, I would like to send my deepest love to my mother Tülin ÇEVİK and my brother Görkem who together endured my various anxiety responses. I would also like to thank to my father to allow me to stand still despite all.

## TABLE OF CONTENTS

# LIST OF TABLES

## LIST OF FIGURES

# CHAPTER 1

# INTRODUCTION

## 1.1. General

Throughout life, old or damaged bone is periodically removed and new bone is formed at discrete sites throughout the skeleton. This regenerative process of bone remodeling is dependent on the coupled formative and resorptive activities of specialized bone cells, osteoblasts and osteoclasts, and serves to prevent inappropriate changes in bone mass allowing precise structural adaptation necessary to meet the varying physical and metabolic demands placed on the skeleton (Spencer et al., 2004).

The activities of bone cells have been reported to be regulated by various systemic and auto/paracrine factors and cellular signals. Such auto- and paracrine factors include cytokines, growth factors and prostoglandins as well as signals of mechanical strain

(Goldring and Goldring, 1996; Martin et al., 1998; Lundberg, P. and Lerner U. H., 2002).

During the last two decades, it has become evident that bone cells also are controlled by the nervous system. Neural regulation of bone metabolism mediated by osteoblastic and osteoclastic cells was demonstrated by clinical and immunohistochemical studies. Clinical observations showed that patients with neurological disorders exhibit localized osteopenia and bone fragility (Gillespie, 1963), altered fracture healing (Freehafer and Mast, 1965) and excessive callus formation (Hardy and Dickson, 1963). Immunohistochemical studies (Bjurholm et al., 1988, 1989; Hill and Elde, 1990, 1991) revealed an extensive network of nerve fibers in the vicinity and within the skeleton (Togari A., 2002). Phenotyping of the skeletal nerve fibers demonstrated the existence of different signaling molecules including neuropeptides, neurotransmitters and neurotrophins in bone tissue (Lundberg and Lerner, 2002). In addition, bone cells express a range of functional neurotransmitter and neuromediator receptors. Based on pharmacological studies and cAMP assays, along with neuropeptide Y (NPY), expression of vasointestinal peptide (VIP1 and VIP2) and calcitonin gene related peptide (CGRP) receptors were demonstrated on osteoblasts (Bjurholm et al,1992; Rahman, S.,et al.1992;

Michelangeli, V.P.et al.1989) and their expression was subsequently confirmed by RT-PCR (Togari, A., et al 1997; Lundberg, P., .et al 2001; Spencer G.J., et al 2004). Their expression and activity provides direct evidence for a complex neurotransmitter and neuromediator mediated network in bone.

Despite these observations depicting abundance of nerves in bone, the biology of skeletal innervation, roles of neuropeptides and signaling pathways have been poorly addressed. Up to now, studies on neuromediators demonstrated to have direct effects on bone tissue. One of these neuromediators, substance P, was found to be a potent bone resorptive factor; CGRP was found to inhibit bone resorption, suppress oseoclastogenesis and increase osteoblast proliferation; VIP has been shown to act on both osteoblasts and osteoclasts (Lerner, 2002). But the role of NPY on bone tissue *via* peripheral nervous system remains to be elusive although its existence in bone tissue and its vasoconstrictive action on peripheral blood vessels are well known (Chenu, C., 2002).

In the peripheral nervous system, NPY is co-released with noradrenaline from sympathetic nerves. Supported by strong evidences, direct action of the sympathetic system on bone results in increased bone mass (Ahmad T. et al, 2004). Stemming from this

idea, we suspect that NPY might had an osteogenic effect on bone tissue.

The aim of our study is to try to reveal the possible effects of NPY in the intramedullary area and its surrounding bone tissue. This will lead to the further understanding of neuromediator mediated neural network and neuromediator signaling pathways in bone. Manipulation of these signaling pathways and understanding of neuromediator action offer therapeutic potential (Spencer, et al., 2004) for the treatment of a wide range of bone disorders by inappropriate and excessive changes in bone formation and/or bone resorption such as osteoporosis.

## 1.2 Literature Survey

### 1.2.1 Bone

Bone is a specialized connective tissue that makes up, together with cartilage, the skeletal system. These tissues serve three functions: (a) mechanical, support and site of muscle attachment for locomotion; (b) protective, for vital organs and bone marrow; and (c)

metabolic, as a reserve of ions, especially calcium and phosphate, for the maintenance of serum homeostasis which is essential to life (Shier, D. et al., 1996).

#### 1.2.1.1. Shapes of Bones

Short bones are cube-like, with their lengths and widths roughly equal. The bones of the wrists and ankles are examples of this type.

Flat bones are plate-like structures with broad surfaces, such as ribs, scapulae and bones of the skull.

Irregular bones have a variety of shapes and are usually connected to several other bones. Irregular bones include the vertebrae that comprise the backbone and many facial bones.

#### 1.2.1.2. Types of Bone Tissue

#### 1.2.1.2.1 Trabecular *versus* Compact Bone

In principle the porosity of bone can vary continuously from zero to 100%. Most bone tissues are of either very low or very high porosity. The two types of bone according to their porosity are referred to as compact bone or trabecular bone, respectively.

Trabecular bone (also called cancellous or spongy bone) is porous bone found in cuboidal bones, flat bones and the ends of long bones; its porosity is 75-95%. The pores are interconnected and filled with marrow. The bone matrix is in the form of plates or struts called trabeculae, each about 200 micrometers thick.

Compact bone is the dense bone found in shafts of long bones and forming a cortex or shell around vertebral bodies and other spongy bones. Its porosity is 5-10 %, and its pores consist of spaces categorized as follows:

Harvesian canals are approximately aligned to the long axis of bone, contain capillaries and nerves, and are about 50 micrometers thick in diameter.

Volkmann's canals are short, transverse canal connecting Harvesian canals to each other and to the outside surface of the bone. These canals also contain blood vessels and probably nerves.

Resorption cavities are the temporary spaces created by osteoclasts in the initial stage of remodeling. Resorption cavities are about 200 micrometers in diameter.

It is important to notice that bone is a dynamic porous structure; its porosity may change as the result of a pathologic condition or in a normal adaptive response to a mechanical or physiological stimulus. Trabecular bone may become more compact or compact bone may become more porous. Such changes strongly affect bone's mechanical properties (Martin, R.B., et al., 1998).

#### 1.2.1.2.2 Lamellar versus Woven Bone

At the microscopic structural level, bone is classified as either woven or lamellar (Kaplan et al. ,1994). Woven, also known as "primary", bone is characterized by random orientation of colagen fibers and non-uniform distribution of cells within that matrix (Kaplan et al., 1994). Compared to woven bone, lamellar bone, which results from remodelling of existing woven bone, has highly organized

collagen fibers and contains fewer cells within its matrix (Kaplan et al., 1994).

#### 1.2.1.2.3. Primary versus Secondary Bone

Compact bone may be further characterized as primary or secondary bone.

Primary bone is tissue laid down de novo on an existing bone surface, such as the periosteal surface, during growth. It may be of two general types:

Circumferential lamellar bone, in which the lamellae are parallel to the bone surface. Blood vessels are incorporated into the lamellar structure such that each is surrounded by several circular lamellae, forming a primary osteon with a primary Harvesian canal at its center.

Plexiform bone, in which the rate of formation is greatly increased by continually constructing a trabecular network on the surface and filling in the gaps. The result is a mixture of woven bone (the trabeculae) and lamellar bone.

Secondary bone results from the resorption of existing bone and almost immediate replacement by new, lamellar bone. This process is known as remodeling. In compact bone, secondary structure consists of cylindrical structures known as secondary osteons or Harvesian systems. These are about 200 micrometers in diameter, and consist of about 16 cylindrical lamellae surrounding a central Harvesian canal. The boundary between the osteon and the surrounding bone is known as the cement line (Martin, R.B., et al., 1998).

### 1.2.1.3. Composition of Bone

Bone is formed by collagen fibers (Type I, 90 % of the total protein) usually oriented in a preferential direction and noncollagenous proteins. Spindle-or plate shaped crystals of hydroxyapatite [$3Ca_3(PO_4)_2$].$(OH)_2$ ] are found on the collagen fibers, within them and in the ground substance. They tend to be oriented in the same direction as collagen fibers. The ground substance is primarily composed of glycoproteins and proteoglycans. These highly anionic complexes have a high ion-binding capacity and are thought to play an important part in the calcification process and the fixation of

hydroxyapatite crystals to the collagen fibers (Favus, J. M. et al., 1999)

### 1.2.1.4. Cellular Organizations within Bone Matrix:

Bone tissue contains four major types of cells: osteoblasts, osteocytes, bone lining cells and osteoclasts. In addition the periost of bone contain fibroblasts, while the vasculature within bone tissue contains endothelial cells (Nagatomi, J. 2002).

#### 1.2.1.4.1. Osteoblasts:

The osteoblast is the bone lining cell responsible for the production of the matrix constituents (collagen and the ground substance). It originates from a local mesenchymal stem cell (bone marrow stromal stem cell or connective tissue mesenchymal stem cell). These precursors, with the right stimulation, undergo proliferation and differentiate into preosteoblasts and then into mature osteoblasts. Osteoblasts never appear or function individually but always found in clusters of cuboidal cells along the bone surface. Osteoblasts are always found lining the layer the layer of bone matrix that they are producing, before it is calcified (called at this point, osteoid tissue). Osteoid tissue exists because of a time lag between

matrix formation and its subsequent calcification (the osteoid maturation period), which is approximately 10 days (Shier, D. et al., 1996).

At the ultra-structural level the osteoblast is characterized by a) presence of an extremely well-developed rough endoplasmic reticulum with dilated cisternae and a dense granular content, b) the presence of a large circular Golgi complex comprising multiple Golgi stacks. The plasma membrane of the osteoblast is also rich in alkaline phosphatase (the concentration of which in the serum is used as an index of bone formation) and has been shown to have receptors for parathyroid hormone but not for calcitonin. The osteoblasts also express steroid receptors for estrogens and vitamin $D_3$ in their nuclei, as well as several adhesion molecules (integrins) and receptors for cytokines. Toward the end of the secreting period, the osteoblast becomes either a flat lining cell or an osteocyte (Shier, D.et al., 1996).

**1.2.1.4.2. Osteocytes:**

The calcified bone matrix is not metabolically inert and cells (osteocytes) are found embedded deep within the bone in small osteocytic lacunae. They were originally bone-forming cells (osteoblasts), which became trapped in the bone matrix that they

produced and which later became calcified. They nevertheless express some specific membrane proteins. These cells have numerous and long cell processes rich in microfilaments, which are in contact with cell processes from other osteocytes (there are frequent gap junctions) or with processes from the cells lining the bone surface (osteoblasts or flat lining cells n the endosteum or periosteum. These processes are organized during the formation of matrix and before its calcification; they perform a network of thin canaliculli permeating the entire bone matrix (Shier, D.et al., 1996). Between the osteocyte's plasma membrane and the bone matrix itself is the periosteocytic space. This space exists both in the lacunae and in the canaliculli, and it is filled with extracellular fluid (ECF) (Shier, D. et al., 1996).

**1.2.1.4.3. Osteoclasts:**

The osteoclast is a giant multinucleated cell, containing four to 20 nucleotide. It is usually found in contact with a calcified bone surface and within a lacuna (Howship's lacunae) that is the result of its own resorptive activity. It is possible to find up to four or five osteoclasts in the same resorptive site, but there usually are only one or two (Favus, J.M., 1999).

#### 1.2.1.4.4. Fibroblasts:

Fibroblasts are the basic type of cells in the connective tissue. These cells synthesize and secrete components of connective tissue extracellular matrix including insoluble collagen (Lodish, et al., 1995). In the skeletal system, fibroblasts are present in the periosteum and are involved in the formation of calluses following fracture of bones (Nagatomi, J., 2002).

### 1.2.2. Skeletal Homeostasis and Bone Mass:

The functions of bones include maintaining blood calcium levels, providing mechanical support to soft tissues and serving as levers for muscle action and supporting hematopoiesis. These functions are accomplished by continuous tissue renewal, called remodeling, occurring throughout life at approximately two million microscopic sites in the adult skeleton (Boyle et al., 2003).

Bone destruction or "resorption" is carried out by haematopoietically derived osteoclasts. Their number and activity is determined by cell lineage allocation, proliferation and differentiation of osteoclast precursors and the resorptive efficiency of mature osteoclasts. (Boyle et al., 2003)

Mesenchyme derived osteoblasts rebuild the resorbed bone by elaborating matrix that then becomes mineralized. Injectable PTH is the only known agent currently available for pharmacological stimulation bone formation (Harada S. and Rodan G., 2003) .

Bone mass in adults is maintained locally by the balance between osteoclastic bone resorption and osteoblastic bone formation, each of which is subject to controls aimed at fulfilling bone function (Harada and Rodan, 2003). Bone resorption and formation are coupled locally by mechanisms not fully understood, that is, when one goes up or down the other usually follows. But resorption is much faster than formation (it takes at least three months to rebuild bone resorbed in 2-3 weeks) (Harada and Rodan, 2003).

### 1.2.3 Neuropeptides and Bone Tissue:

The role of peptides as signaling molecules in the nervous system has been studied for more than 30 years. Over the past 25 years, numerous studies revealed that peptides are also messengers in the nervous system (Hökfelt et al. , 2003) .A peptide secreted by neurons that functions as a signaling molecule either at a synapse or

elsewhere is called a neuropeptide (Lodish et al., 2001). Another definition is made by Holmgren and Jensen (2001) as "neuropeptide is a peptide that can be released from a neuron as signaling molecule". Neuropeptides and their G-protein coupled receptors are widely distributed throughout the body. They commonly occur with and are complementary to classical neurotransmitters. The substances that mediate neuronal activity after secreted from nerve tissue are called neuromediators (either neuropeptides or another substance). Actually they can be encountered in every point that nervous system reaches –the brain, spinal cord, gastrointestinal tract, autonomic and sensory glia. However, each peptide has its unique distribution pattern (Lundberg, 1996).

Although coexistence of neuropeptide with neurotransmitters seems to be inevitable, some distinct features that neuropeptides differ from classical neurotransmitters. The mode of synthesis and replacement after release are the principal differences. Classic neurotransmitters often have a membrane re-uptake mechanism through specific transporter molecules which allow reutilization of the transmitter (Lundberg, 1996).

The existence of neuromediators in bone was shown through the ends of the 1980s (Bjurholm et al., 1989). In the following years,

bone tissue was shown to host neuropeptides and their receptors *via* histochemical staining. Bjurholm stressed that these receptors of interest were especially existing on epiphyseal cartilage and periosteum regions which were both known to be hosts of intense osteogenic activity . This implied that neural tissue and bone tissue are not that much isolated apart and there exists neuroendocrine effect in the bone physiology (Bjurholm, 1991). In a study with rats, Hill and Elde stained the long bones with immunohistochemical techniques and revealed that the diaphysis of long bones contains more nerve endings than epiphysis. Consequently, they claimed that nerve endings belonged to sympathetic nervous system (Hill and Elde, 1991). In addition to these researchers, Ahmed and Lindbald later proved the existence of autonomous nervous system *via* displaying the occurrence of neuropeptides in the bone tissue (Ahmed et al., 1994; Lindbald et al., 1994). Again Ahmed and his coworkers extracted various neuropeptides (including NPY) and quantified them *via* radioimmunoassay technique. They concluded that neuropeptides have effects on nosiception, vasoactivity, immune function and various bone metabolism activity in the bone tissue (Ahmed et al.,1994). Sisask et al. (1996) revealed that neuropeptides have active role in the bone development and growth.

NPY belongs to the pancreatic polypeptide family (PP), so named after a peptide found during the process of isolating insulin pancreatic islets. All members of the family ( NPY, PYY, PP, PY) consists of 36 amino acid residues and have a carboxyterminal amide (Thorsell A. and Heilig M., 2002).

The expression of NPY is upregulated by glucocorticoids, cAMP elevation and protein kinase activation and prepro-NPY gene has been highly conserved during evolution. A high amino acid sequence homology thus exists between NPY from different species and rat NPY are identical to human NPY. NPY has proven to take various roles in anxiety-related behaviors, feeding behavior and cardiovascular metabolism, memory function and modulation of seizure activity as well as bone metabolism (Lindbald et al., 1994).

Immunohistochemical screening of bone tissue has revealed the presence of NPY co-localized with norepinephrine in vascular nerve fibers, predominantly in the epiphyseal marrow, periosteum, and along the osteochondral junction at the growth plates (Lindbald et al., 1994).

### 1.2.4. Biomechanics of Bone:

Although bone densitometry is often used as a surrogate to evaluate bone fragility, direct biomechanical testing of bone undoubtedly provides more information about mechanical integrity. Like any other specialized field, biomechanics contains its own techniques and vocabulary (Turner C.H. and Burr D.B,1993).

To determine the mechanical properties of a structure -or, more typically, a major part of a structure, such as the shaft of a femur- engineers conduct a load-deformation test. The structure is loaded in a manner appropriate for its actual function- tension, compression, torsion or bending- and its deformation is recorded as a function of the applied load- a load deformation curve is obtained. Typically, load and deformation are linearly proportional for some time until the proportional limit is reached; then the slope of the load-deformation curve is reduced (Martin, R. B et al, 1998).

The concepts of stress and strain are fundamental to bone biomechanics. When a force is applied to any material, such as bone, it deforms. The amount of deformation in the material, relative to its original length is the strain. Strain is a dimensionless unit formally defined as the change in length divided by its original length ($\varepsilon$ =

$\Delta L/L$). When a material is pulled it gets longer (tensile strain). When a material is pushed together, the material shortens (compressive strain). Shear strain is the angle , measured in radians, through which a material has been deformed by forces acting parallel rather than opposed to the material. Shear strain arises when layers of a material slide against another, as might occur with torsion or bending (Favus, J. M, et al., 1999)

A load-deformation curve may be converted to a stress-strain curve by using appropriate formulas to change load to stress and deformation to strain. For example, in a compressed bone shaft, the load is divided by the cross-sectional area of the bone cortex to obtain stress, and the deformation is divided by the original length of the shaft segment to obtain strain. The slope of the linear region is the stiffness of the material. For normal loading (tension or compression) the material stiffness is known as the elastic modulus or Young's modulus. Young's modulus has the same units as stress, and values for bone are typically in the order of mega ($10^6$ pascals) or gigapascals ($10^9$ pascals) ( Martin, R. B et al, 1998).

The degree to which a material deforms depends not only on the magnitude of the forces and moments (turning, twisting or rotational effects of a force) but also on the stiffness of the constituent

materials. In the case of bone, stiffness is determined by the relative proportions of hydroxyapatite crystals and the collagen fibers that make up the composite (Favus J.M.,1999)

During the initial stages of any test to define a bone's material properties, there is a linear increase in the strain as the stress increases. This is known as the elastic region. Should the load removed during this phase of the test, the specimen will return to its original size and shape almost immediately without incurring permanent damage. The linear relation between strain and stress is called Hooke's Law ($E= \sigma/\varepsilon$; where E is elastic modulus). This law relates one component of stress to its corresponding strain component (e.g., stress and strain in longitudinal tension), and it applies only to the linear portion of the stress-strain curve between the origin and the proportional limit (Martin R. B., et al ,1998).

The slope of the elastic region of the stress-strain curve reflects the stiffness of the material, otherwise known as the modulus of elasticity. The stiffer the material the steeper the slope of the line (Martin R. B., et al ,1998).

Among many biomechanical testing methods, bending tests are useful for measuring the mechanical properties of bones from

rodents and other small animals. In the bending test the whole bone is loaded in bending until failure. Bending causes tensile stresses on one side of the bone and compressive stresses on the other. Bone is weaker in tension than compression, so in a bending test failure usually occurs on tensile side of the bone (Turner C.H. and Burr D.B, 1993).

Bending can be applied to the bone using either three-point or four point loading (Turner C.H. and Burr D.B, 1993).

Three point bending test has commonly been used in the evaluation of bone studies bone strength in earlier studies, which have shown that bending breaking force (breaking or fracture load) and stiffness, as well as the intrinsic parameters (breaking strength) and elastic modulus are good indicators of the mechanical strength of cortical bone (Jamsa et al, 1998).

### 1.2.5 Basic Definitions in Bone Densitometry

The material properties of bone are frequently discussed in terms of its "density". Used alone, this word would be expected to

refer to the specific gravity of the solid matrix. The term apparent density, on the other hand refers to the mass per unit volume of a region of bulk bone, which includes Harvesian canals, marrow spaces, and other soft tissue spaces. Therefore, apparent density is a function of both the porosity and mineralization of the bone mineral (Martin R.B, et al, 1998).

Bone mineral density is a test that measures the amount of bone mineral, calcium hydroxyapatite, on a specific region of a bone per unit area or volume. From this information, an estimate of the strength of a bone specimen can be made by using relations developed by Carter and Hayes (1977) or Rice et al (1988).

There are several methods of noninvasively measuring bone mass, that is, the amount or density of bone in a particular part of the skeleton. Most of these methods depend on the absorption of photons by the bone, and because the mineral absorbs photons much more readily than the collagen, water, and soft tissues, these methods essentially measure bone mineral. However, because the variability of mineralization in adult bones is much less than that of porosity, these methods provide information about adult bone size and porosity as well (Martin R.B, et al, 1998).

The oldest and simplest of these methods is a simple radiographic film or "X-ray". However, from variability in exposure and processing, a 30-50 % reduction in bone density may occur without being evident on a standard clinical radiograph. Quantitative computed tomography images are considerably more accurate, but both these methods involve significant radiation doses. In the 1970s, this problem was significantly reduced by the development of photon absorptiometry by Mazess and Cameron (1972). This method involves scanning across a bone with a beam of photons emitted from a low level radionuclide such as $^{125}I$. The source is fixed opposite to a detector, the beam is scanned across the bone, and the intensity of the radiation received by the detector, *I*, is plotted as a function of scan position, x. The area within the resulting absorption curve is proportional to the mineral content of the bone in the path of the beam. Results are reported as bone mineral content (BMC, g mineral/cm bone length) and bone mineral density (BMC/bone width, g mineral/cm bone length). Later, it was realized that by scanning with two radionucleotides emitting photons with different absorption coefficients, correction could be made for the fact that soft tissues absorb some radiation; this is known as *dual energy photon absorptiometry* (Martin R.B, et al, 1998).

The development of bone densitometry has certainly been driven by the need to overcome the inherent short comings of plain radiography for assessing bone density. Conventional X-ray radiography can not detect mild loss in bone density. In addition, conventional radiography does not measure cancellous bone and does not recognize bone loss within the cortex.

In the 1990s, an alternative version of this known as *dual energy x-ray absorptiometry* (DEXA or DXA) was developed. DEXA was developed to measure bone mineral at multiple sites This technique substitutes low energy X-rays for the radionuclide source, and involves scanning back and forth along some of the bone to produce a two dimensional image. These widely used absorbtiometry methods are accurate to within 1%-2% and expose the patient to a fraction of the radiation dose of standard chest X-ray. By analyzing photon absorption at two different energies, one can calculate the amount of bone mineral, soft tissue, and fat without need to have constant body-part thickness. The major advantage of DEXA is its ability to measure skeletal density at sites rather than the extremities, especially in the lumbar spine and proximal femur. For adequate evaluation of overall bone mineral status, both cortical and trabecular sites should be examined separately (Favus, J.M, et al., 1999)

In comparison to conventional radiography, computed tomography scanners generate cross-sectional images of the object by measuring the attenuation of a beam of X-rays as it is rotated around the object at angular increments within a single plane. From a set of these measurements, Fourier transform algorithms are used to reconstruct a cross-sectional image (Akın, S. and Kovscek, A.R., 2003).

Quantitative computed tomography (QCT) is an excellent technique to determine a three dimensional measurement of existing bone mass. QCT assesses volumetric density ($g/cm^3$) rather than two dimensional area density ($g/cm^2$) generated from a DEXA scan. QCT offers the most sensitive measuring method; however the technology is costlier and associated with higher amounts of radiation exposure. QCT has proven to be an effective tool in evaluating the densitometric and geometric properties of human bones. It also been used in experimental studies on rat bones. (Jamsa, T. et al., 1998).

# CHAPTER 2

# MATERIALS AND METHODS

## 2.1. Animals and Surgery:

Male Wistar rats (average weight N= 350 ± 50 g, average age M= 4 ± 0.5 months) were obtained from Pamukkale University Faculty of Medicine Animal Care Unit (Denizli, TURKEY). The total number of 28 male Wistar rats were divided into three subgroups according to the time points of evaluation: (a) day one, (b) week one and (c) week two. For each time point, (a) HA, (b) NPY dose 1, (c)NPY dose 2 and (d) NPY plus NPY inhibitor were injected to the right tibia of each rat. In order to inject the chemicals, a single defect of 3 mm diameter was created with a surgical drill. Day one groups consisted of one rat per group, and week one and week two groups consisted of three rats per group. Rats were caged in METU Engineering Sciences Department Animal Care Laboratory. The laboratory temperature was kept at 23 (±1) °C and at 50 % (±10) humidity with controlled air conditioning system. Artificial day and night effect was created on a 12-hour light/dark regular household fluorescent lights. Adequate amount of food pellets and water were provided. Regular cleanings and

disinfection of cages and living environment were secured. In order to ensure acclimatization, the earliest surgery was carried at least one week after the transfer of rats to the animal care unit. At most three male rats were allowed to share one cage that allowed them to move freely in a standard cage. Food and water were provided from the top of the cages so that rats were made use their hind limbs to carry their body weight when they recovered (inside cage feeding is applied for the day one group and for the first three days after the surgery in all groups. All procedures were fully compliant with Turkish law (number 6343/2), Veterinary Medicine Deontology Regulation 6.7.26 and with the Helsinki Declaration of Animal Rights.

Anesthesia was induced with an intraperitoneal injection of 15 mg/kg ketamine (Alfamine, Alfasan Int., Netherlands). The $1x10^{-5}$ M NPY (Sigma Chemicals, 1 mg, NPY-recombinant) was designated as NPY dose 1 and $1x10^{-6}$ M NPY was designated as NPY dose 2. Both doses were dissolved in appropriate volume of hyaluronic acid (Adant, 2.5 ml, Meiji Seika Kaisha, Japan). From these stock preparations, 0.1 ml of aliquots were applied to each rat. Only HA injected rats constituted the control group (designated as HA). The group that is designated as NPY plus inhibitor was composed of NPY dose2 plus NPY inhibitor (Sigma Chemicals, 1mg, Neuropeptide Y

antagonist). The drilled injection zones were covered with bone wax (Braun Aesculap AG, Germany). The skin was closed with 4/0 monoflament nylon material (Prolene, Ethican C.,USA).

Rats were executed by overdose anesthetic application at the end of the study. The right tibia were removed and kept at –20 °C for the analysis.

**2.2 Conventional Radiography:**

The integrity of the specimens and possible new bone formation were evaluated by conventional radiography. Two experts evaluated the X-rays independently.

Radiography images were obtained at METU Medical Center with a Siemens, Multi-C Radiography Machine. Graphics were gathered at 44kV and 3.2 m As /s. The distance between the X-ray source and bone specimens was fixed at 100 cm. Agfa Crurix radiograph films and Agfa Crurix 60 automatic film developing machine was used to obtain the image.

## 2.3. Bone Density Measurements Using Dual X-Ray Absorbtiometry (DEXA):

The tibia specimens were placed in a water bath, and their anterior surfaces faced up with respect to the vertical to the X-ray source. The bath was filled with distilled water up to 2 cm above the tibial surface. The X-ray beam composed of two energy levels, which was absorbed differently by the bones. These levels were 76 kVp and 140 kVp, both having 2.0 mA and 60 Hz. Since the analysis is small animal bone density analysis, resolution of DEXA was set to detailed mode in which single scan time extended to 3.5 minutes. Density values in g/ $cm^2$ were recorded for each group.

## 2.4 Quantitative Computer Tomography (QCT):

QCT performs cross-sectional imaging of an object based on radiography principles. The principle underlying QCT measurements in our study is that new bone formation (calcified tissue) absorbs more x-rays than surrounding tissue. Radiation emission during imaging is greater than DEXA and allows three dimensional analysis of bone density for both medulla and cortex including atomic content of the analyzed section.

The densities and atomic content of the tibia are evaluated using Philips Tomoscan Computer Tomography 60/TX 3 at the Petroleum Research Laboratory (PAL), Petroleum and Natural Gas Engineering Department, METU.

All test specimens were placed inside plastic "falcon" tubes containing isotonic saline solution. Prepared specimens were fixed 60 cm away from the X-ray source on the Tomoscan table.

During CT examinations, 576 channel detectors were present to sense 100 kV and 130 kV energy discharges. The time needed to complete one full cross-sectional imaging of the test specimen was 3 seconds. The distance between two cross sectional images was 2 mm. Field of view was 300 mm and field length was 4mm. The current flow through the X-ray source was 250 mA.

All captured images were transferred into Intel Pentium 4 powered image analysis software and calculations were performed by "CT Density Calculator" software developed by using Visual Basic 6.0 programming language by Ömer İZGEÇ. From the captured images, this program was able to calculate atomic content and density for both medulla and cortex of the bone.

## 2.5 .Three Point Bending Test:

Tests were performed at the Biomechanics Laboratory, Engineering Sciences Department, METU. Before mechanical experiments, tibia specimens were thawed to room temperature for 2 hours. Adhered soft tissue surrounding the bones and the callus were carefully removed. Dimensional properties of each tibia were recorded.

Changes in bone strength as a result of new bone formation or possible bone loss were determined by three point bending test.

Each tibia were placed to the supporting table at their two endpoints. The force was exerted on the mid tibia through Lloyd LS 500 Material Testing Machine (Southampton, UK). Cross-head speed was 3 mm/min. All three-point bending results were stored at 3.3.Hz by a connected PC. Results were displayed as load-deformation curve. Load-deformation curve of each tibia specimen was converted to stress-strain curve as mentioned in part 1.2.4. From this graph, Young's modulus (E) for each tibia specimen was obtained and accepted as data.

## 2.6. Histological Evaluation:

Tibia samples collected according to their time points were allowed to fix in 10% formaldehyde and stored until they were evaluated for histology. Then, they were decalcified gradually by placing into Decastro solution at room temperature. Decastro solution was consisted of absolute ethanol (300 ml), chloraldehyde 50g, DW 670 ml, nitric acid (concentrated –70%) of 30 ml. After decalcification, gradual alcohol treatment was applied for dehydration and constant vacuum application was performed. Then the specimens were embedded into paraffin blocks. From paraffin blocks, 4-6 micro meters thick sections were taken with a rotary microtome (Microm, HM 360, Germany). Histological sections were stained with the Hematoxylin and Eosin and Goldner's Masson trichrome technique. Stained specimens primarily evaluated from the aspects of tissue repair related new bone and bone marrow formation.

## 2.7. Statistical Analysis:

All measurements were expressed as means and standard deviations. Data were analyzed using two way analysis of variance to asses statistical significance. Independent variables were groups of subjects (four levels; HA, NPY dose 1, NPY dose 2, NPY-plus

inhibitor) and time period ( three levels; first day, first week and second week); dependent variables were DEXA measurement, QCT based density of cortex, QCT based density of medulla, QCT based atomic content of cortex, QCT based atomic content of medulla, three point bending test results. SPSS 8.0 program was used for these statistical analysis.

# CHAPTER 3

# RESULTS AND DISCUSSION

## 3.1. Findings of Conventional Radiography:

No significant differences were observed in the conventional radiological data between the groups. Fractured specimens were excluded from further tests using this evaluation. Radiographic image of all groups were gathered together on one image (see appendix).

## 3.2. Findings of DEXA Analysis:

Result of the analysis revealed that there was no significant interaction effect between group of subjects and time points in terms of DEXA measurements (Table 3.1, Figure 3.2.1). However, there was a group main effect ($F(3,16)=6.7$, $p=0.004$) that is, to say, there was significant difference between group of subjects. Tukey test was used as post hoc analysis to assess pairwise differences. Result of the analysis revealed that the mean of NPY dose 1 ($X=0.13$) was significantly lower than HA ($X=0.18$).

Although it was statistically not significant, the NPY plus inhibitor applied tibia specimen was found to have lower bone density than the control group. Bone density of the inhibitor applied specimen increased in the following two weeks compared to an initial decrease on the first day. NPY dose 2 group had also higher bone density than NPY dose 1 group.

**Table 3.1 Descriptive Statistics of DEXA Results**

**Descriptive Statistics**

| time point | group of subject | Mean | Std. Deviation | N |
|---|---|---|---|---|
| first day | npy1 | ,1300 | . | 1 |
| | npy2 | ,1500 | . | 1 |
| | inhib | ,1000 | . | 1 |
| | ha | ,1900 | . | 1 |
| | Total | ,1425 | 3,775E-02 | 4 |
| first week | npy1 | ,1233 | 5,774E-03 | 3 |
| | npy2 | ,1567 | 1,155E-02 | 3 |
| | inhib | ,1500 | 3,606E-02 | 3 |
| | ha | ,1633 | 5,774E-03 | 3 |
| | Total | ,1483 | 2,290E-02 | 12 |
| second week | npy1 | ,1367 | 3,786E-02 | 3 |
| | npy2 | ,1533 | 1,155E-02 | 3 |
| | inhib | ,1733 | 2,082E-02 | 3 |
| | ha | ,2033 | 1,528E-02 | 3 |
| | Total | ,1667 | 3,284E-02 | 12 |
| Total | npy1 | ,1300 | 2,309E-02 | 7 |
| | npy2 | ,1543 | 9,759E-03 | 7 |
| | inhib | ,1529 | 3,546E-02 | 7 |
| | ha | ,1843 | 2,225E-02 | 7 |
| | Total | ,1554 | 3,024E-02 | 28 |

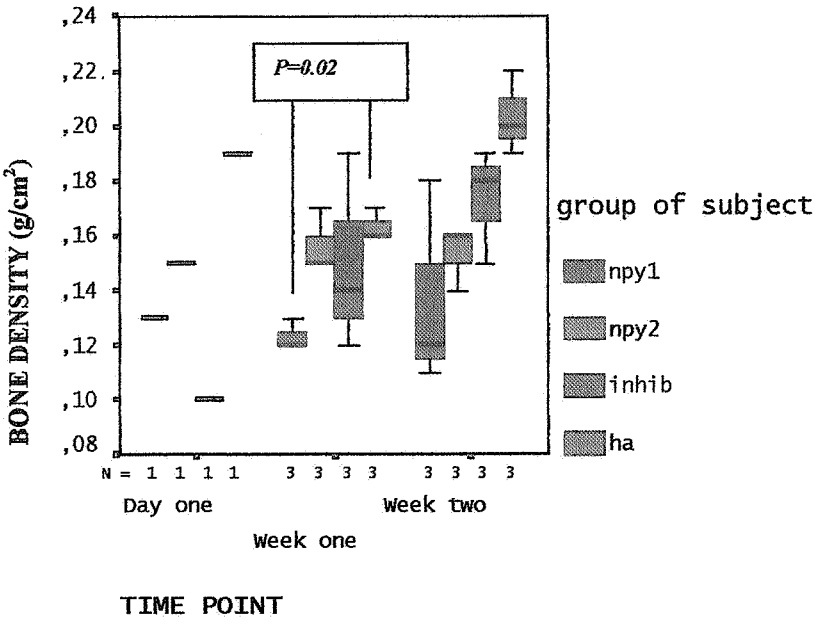


**Figure 3.2.1 Profile Plot of DEXA Analysis:** Y-axis displays bone density in g/cm2 and X-axis displays time point and N stands for number of rats analyzed. Group of subjects are displayed in different colors.

### 3.3. Cortex Density Measured By QCT:

A time and group main effect ($F(2,16)=14.6$), $P=0.00$; $F(3,16)=6.02$, $P=0.006$, respectively) was observed in cortex density measured by QCT (Table 3.2) (Figure 3.2.2). However, there was no time and group interaction effect. Result of post-hoc analysis revealed

that mean of day one (X=1.8) was significantly lower than the mean of week one ( X=1.9) and the mean of week two (X=2.02). These findings were parallel to the DEXA findings.

**Table 3.2 Descriptive Statistics of Cortex Density Measured By QCT**

**Descriptive Statistics**

| time point | group of subject | Mean | Std. Deviation | N |
|---|---|---|---|---|
| first week | npy1 | 64,6600 | 11,8794 | 2 |
| | npy2 | 45,5500 | 25,4700 | 2 |
| | inhib | 49,2100 | 39,1030 | 2 |
| | ha | 13,6400 | , | 1 |
| | Total | 47,4971 | 26,0377 | 7 |
| second week | npy1 | 124,5000 | 101,8234 | 2 |
| | npy2 | 31,4350 | 23,9073 | 2 |
| | inhib | 36,0600 | 15,1604 | 2 |
| | ha | 44,2900 | , | 1 |
| | Total | 61,1829 | 61,2441 | 7 |
| Total | npy1 | 94,5800 | 68,5321 | 4 |
| | npy2 | 38,4925 | 21,7525 | 4 |
| | inhib | 42,6350 | 25,3759 | 4 |
| | ha | 28,9650 | 21,6728 | 2 |
| | Total | 54,3400 | 45,7656 | 14 |

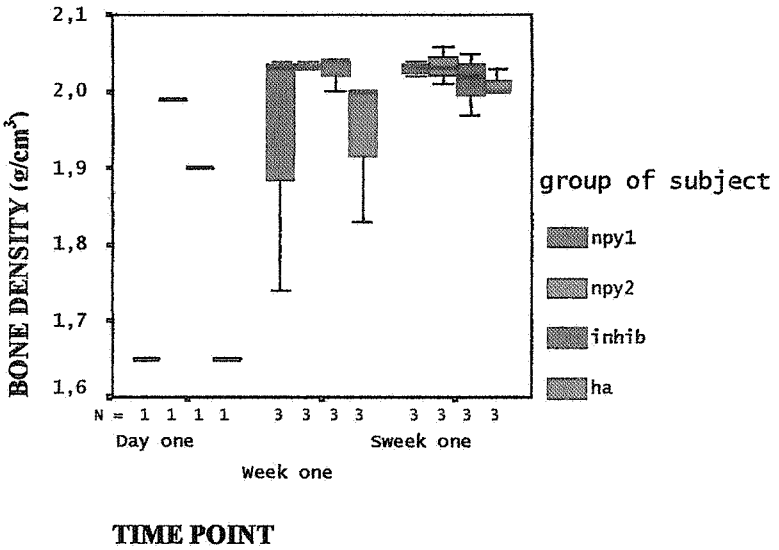


**Figure 3.2.2 Profile Plot of Cortex Density Measured By QCT:** Y-axis displays bone density of cortex in g/cm3, X-axis displays time points and N (number of subjects). Groups of subjects are displayed in different colors.

### 3.4. Medullary Density Measured by QCT:

There was a significant time and group interaction effect (F(5,16)=3.4, p=0.02) when the medullary density was measured by QCT (Table 3.3)(Figure 3.2.3). That is to say at day one, the mean of HA (X=1.3) was significantly lower than the mean of NPY dose 2 (X=1.7). Medullary QCT density measurement revealed the same finding as QCT cortex analysis.

**Table 3.3. Descriptive Statistics of Medullary Density Measured By QCT:**

**Descriptive Statistics**

| time point | group of subject | Mean | Std. Deviation | N |
|---|---|---|---|---|
| first day | npy2 | 1,7100 | , | 1 |
| | inhib | 1,5500 | , | 1 |
| | ha | 1,2900 | , | 1 |
| | Total | 1,5167 | ,2120 | 3 |
| first week | npy2 | 1,6100 | ,1552 | 3 |
| | inhib | 1,5567 | 6,028E-02 | 3 |
| | ha | 1,7567 | 7,024E-02 | 3 |
| | npy1 | 1,6867 | ,1007 | 3 |
| | Total | 1,6525 | ,1186 | 12 |
| second week | npy2 | 1,6267 | 6,429E-02 | 3 |
| | inhib | 1,6800 | 5,568E-02 | 3 |
| | ha | 1,6500 | ,1500 | 3 |
| | npy1 | 1,6433 | 3,786E-02 | 3 |
| | Total | 1,6500 | 7,793E-02 | 12 |
| Total | npy2 | 1,6314 | ,1033 | 7 |
| | inhib | 1,6086 | 8,194E-02 | 7 |
| | ha | 1,6443 | ,1908 | 7 |
| | npy1 | 1,6650 | 7,204E-02 | 6 |
| | Total | 1,6363 | ,1176 | 27 |

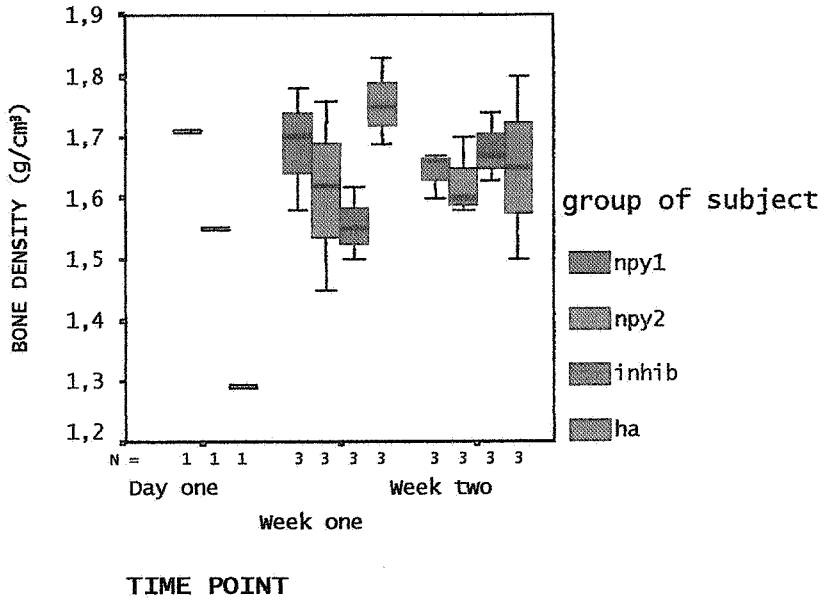


**Figure 3.2.3 Profile Plot of Medullary Density Measured By QCT:.** Y-axis displays bone density of cortex in g/cm3, X-axis displays time points and N (number of subjects). Groups of subjects are displayed in different colors.

### 3.5. Atomic Content of Cortex of Tibia Measured By QCT:

Results of the variance analysis revealed that there was no significant interaction effect. However, there was a group and time point main effect ($F(2,16)=12.3$, $p=0.001$; $F(3,16)=4.6$, $p=0.01$, respectively (Table 3.4) (Figure 3.2.4). The result of the post hoc analysis revealed that the mean of day one data ($X=12.3$) was significantly lower than the mean of week one ($X=12.5$) and the mean

of second week (X=12.5). In terms of group variable, the mean of HA (x=12.4) was significantly lower than the mean of NPY dose 2 (X=12.5).

**Table 3.4 Descriptive Statistics of Atomic Content of Cortex of Tibia Measured By QCT:**

Descriptive Statistics

| time point | group of subject | Mean | Std. Deviation | N |
|---|---|---|---|---|
| first day | npy1 | 12,1800 | . | 1 |
| | npy2 | 12,4600 | . | 1 |
| | inhib | 12,3600 | . | 1 |
| | ha | 12,1800 | . | 1 |
| | Total | 12,2950 | ,13892 | 4 |
| first week | npy1 | 12,4133 | ,15885 | 3 |
| | npy2 | 12,5033 | ,00577 | 3 |
| | inhib | 12,4967 | ,02309 | 3 |
| | ha | 12,4133 | ,09815 | 3 |
| | Total | 12,4567 | ,09218 | 12 |
| second week | npy1 | 12,5000 | ,01000 | 3 |
| | npy2 | 12,5033 | ,02517 | 3 |
| | inhib | 12,4833 | ,04041 | 3 |
| | ha | 12,4800 | ,01732 | 3 |
| | Total | 12,4917 | ,02443 | 12 |
| Total | npy1 | 12,4171 | ,14580 | 7 |
| | npy2 | 12,4971 | ,02215 | 7 |
| | inhib | 12,4714 | ,05640 | 7 |
| | ha | 12,4086 | ,12075 | 7 |
| | Total | 12,4486 | ,10098 | 28 |

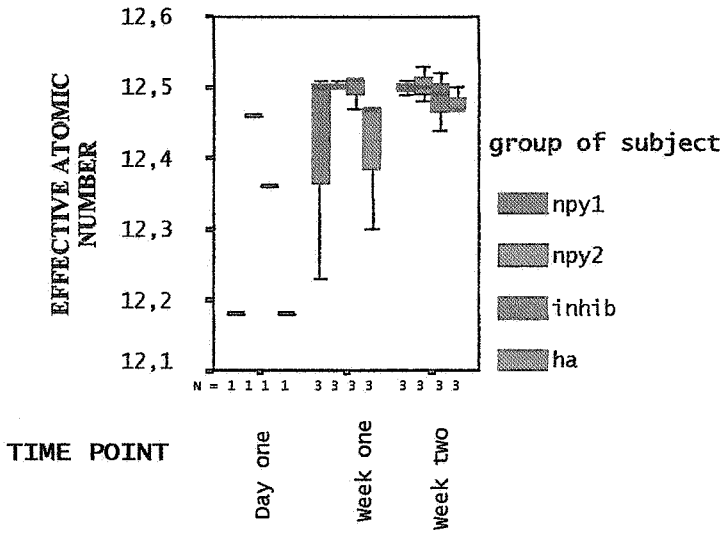


**Figure 3.2.4 Profile Plot of Atomic Content of Cortex of Tibia Specimens.** Y-axis displays effective atomic number (dimensionless), X-axis displays time points and N (number of subjects). Groups of subjects are displayed in different colors.

### 3.6. Atomic Content of Medulla of Tibia Measured By QCT:

There was no significant effect between group of subject and time point in terms of atomic content of medulla measurements. Additionally there was no significant time and group main effect of atomic content. However, from the bar graphs it was observed that medullary atomic content of inhibitor applied tibia specimens

increased by time although the NPY administered specimens' medullary atomic content did not change.

**Table 3.5 Descriptive Statistics of Atomic Content of Medulla of Tibia Specimens**

Descriptive Statistics

| time point | group of subject | Mean | Std. Deviation | N |
|---|---|---|---|---|
| first day | npy1 | 12,1756 | . | 1 |
| | npy2 | 12,2109 | . | 1 |
| | inhib | 12,1315 | . | 1 |
| | ha | 12,0936 | . | 1 |
| | Total | 12,1529 | ,05119 | 4 |
| first week | npy1 | 12,2026 | ,05887 | 3 |
| | npy2 | 12,1704 | ,07066 | 3 |
| | inhib | 12,1361 | ,02244 | 3 |
| | ha | 12,2459 | ,05180 | 3 |
| | Total | 12,1887 | ,06253 | 12 |
| second week | npy1 | 12,1730 | ,01901 | 3 |
| | npy2 | 12,1662 | ,03349 | 3 |
| | inhib | 12,1943 | ,03357 | 3 |
| | ha | 12,1894 | ,08089 | 3 |
| | Total | 12,1807 | ,04253 | 12 |
| Total | npy1 | 12,1861 | ,03895 | 7 |
| | npy2 | 12,1744 | ,04798 | 7 |
| | inhib | 12,1604 | ,03943 | 7 |
| | ha | 12,1999 | ,07794 | 7 |
| | Total | 12,1802 | ,05258 | 28 |

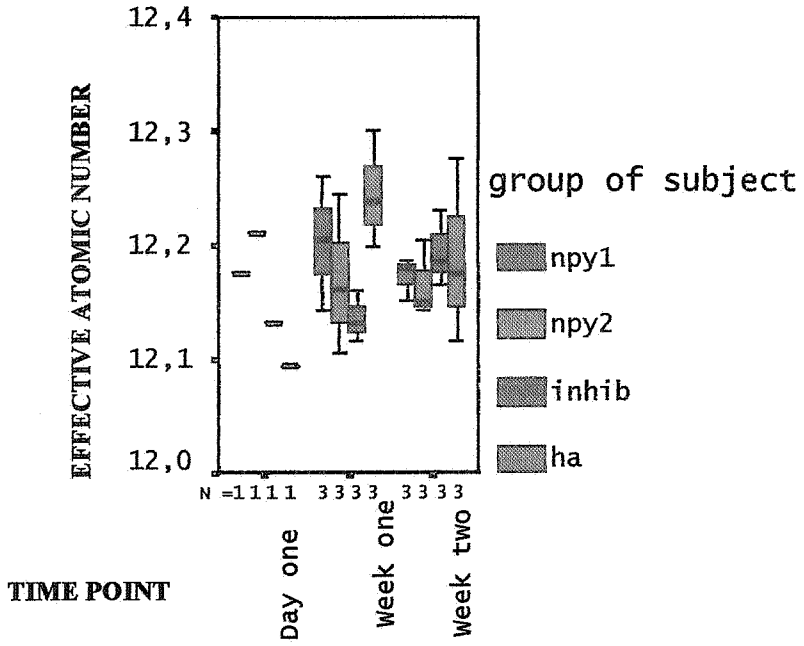


**Figure 3.2.5 Profile Plot of Atomic Content of Medulla of Tibia Measured by QCT**. Y-axis displays effective atomic number (dimensionless), X-axis displays time points and N stands for number of subjects. Groups of subjects are displayed in different colors.

### 3.7. Findings of Three Point Bending Test:

There was no significant effect between group of subject and time point in terms of three point bending tests (Table 3.6)(Figure 3.2.6). Additionally there is no significant time and group main effect on three point bending test.

**Table 3.6 Descriptive Statistics of Three Point Bending Test Data**

**Descriptive Statistics**

| time point | group of subject | Mean | Std. Deviation | N |
|---|---|---|---|---|
| first week | npy1 | 64,6600 | 11,8794 | 2 |
| | npy2 | 45,5500 | 25,4700 | 2 |
| | inhib | 49,2100 | 39,1030 | 2 |
| | ha | 13,6400 | . | 1 |
| | Total | 47,4971 | 26,0377 | 7 |
| second week | npy1 | 124,5000 | 101,8234 | 2 |
| | npy2 | 31,4350 | 23,9073 | 2 |
| | inhib | 36,0600 | 15,1604 | 2 |
| | ha | 44,2900 | . | 1 |
| | Total | 61,1829 | 61,2441 | 7 |
| Total | npy1 | 94,5800 | 68,5321 | 4 |
| | npy2 | 38,4925 | 21,7525 | 4 |
| | inhib | 42,6350 | 25,3759 | 4 |
| | ha | 28,9650 | 21,6728 | 2 |
| | Total | 54,3400 | 45,7656 | 14 |

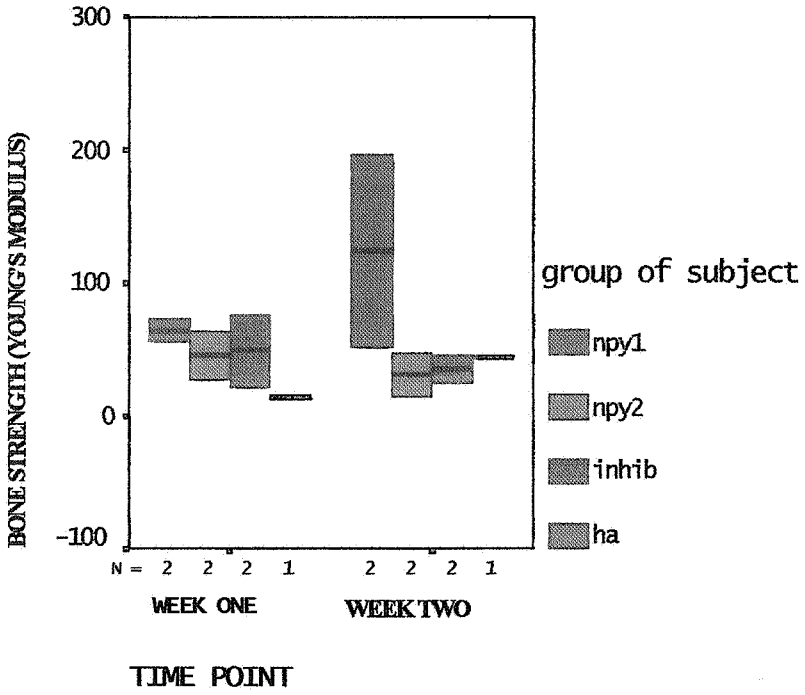


**Figure 3.2.6 Profile Plot of Three Point Bending Test Data**. Y-axis displays bone strength as Young's modulus (dimensionless), X-axis displays time points (biomechanical analysis of day one data was not performed) and N stands for number of subjects. Groups of subjects are displayed in different colors.

### 3.8. Findings of Histology:

In all of the specimens analyzed, from week one to week two, HA degraded simultaneously with the organization of fibrous tissue. Neighboring bone tissue seemed to experience remodeling in its cortex and spongiosa as well as bone medullary elements.

HA was found to be biocompatible with the tissue specimens. The granules belonging to HA were found to be filling all medullary area on the day one, but at the end of the week one they were found to be surrounded by some type of fibrous tissue containing mononuclear inflammatory cells. In the following weeks, this infiltration dominated by lymphocytes and macrophages, was replaced with a fibrous tissue composed of fibroblasts and collagen fibrils. This fibrous collagen tissue was consistent with bordering bone medullary elements which were restoring themselves. In the areas neighboring cortical bone, collagenous fibrils and veins, with the primary bone cells, merged into both doses of NPY loaded HA granules. HA applied specimens did not reveal any foreign object giant macrophage in any sections.

At the end of the day one and week one, NPY and NPY plus inhibitor groups defect healing did not show any significant difference

with respect to the HA group (Figure 3.7.A-J). In both NPY and NPY plus inhibitor groups, inside the defect cavity, HA granules were observed in an almost filling manner (Figure 3.7.A-F). On the 14$^{th}$ day, NPY-HA and only HA applied groups did not reveal any significant difference in terms of bone healing and tissue response to the system. But NPY plus inhibitor application revealed young spongiosis bone trabecules in the borderline of cortical bone as a green thin layer when stained with Masson trichrome technique (Figure 3.7.J).

During the week one, intramedullary areas where injection was applied was fully covered with hyaluronic acid.

The granules of HA were observed to allow formation of fibrous tissue by degrading/resolving itself gradually from periphery to the center. Existence of low number of macrophages and lymphocytes were observed in the collagen tissue surrounding HA granules that were resolving. None of the specimens that were analyzed revealed neutrophils or giant macrophage cells.

On the 14$^{th}$ day of analysis, the experiment and control groups new bone spicules seemed in a positional oppose to each other with the osteoblasts that were on the surface of these spicules. Osteoclasts seemed to sculpt the newly formed bone trabecules to

enhance the development of bone marrow elements inside them. Despite this continuos remodeling process, HA gel and fibrous tissue in between seemed to still reside. Again in this period, healing of bone did not seem doing better than the control (HA) group (Figure 3.1.G-J).

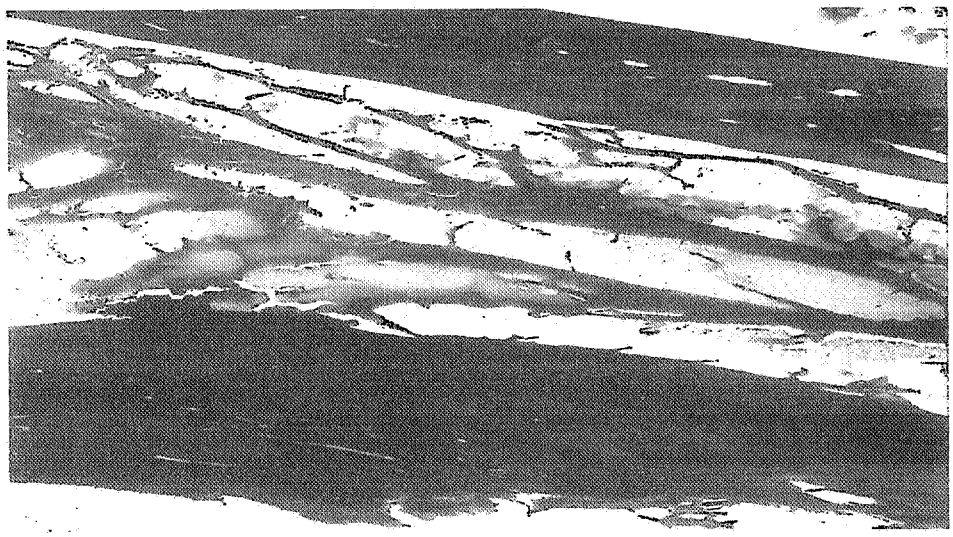

**Figure 3.7.A HA, 1st day, x50 , MT staining**

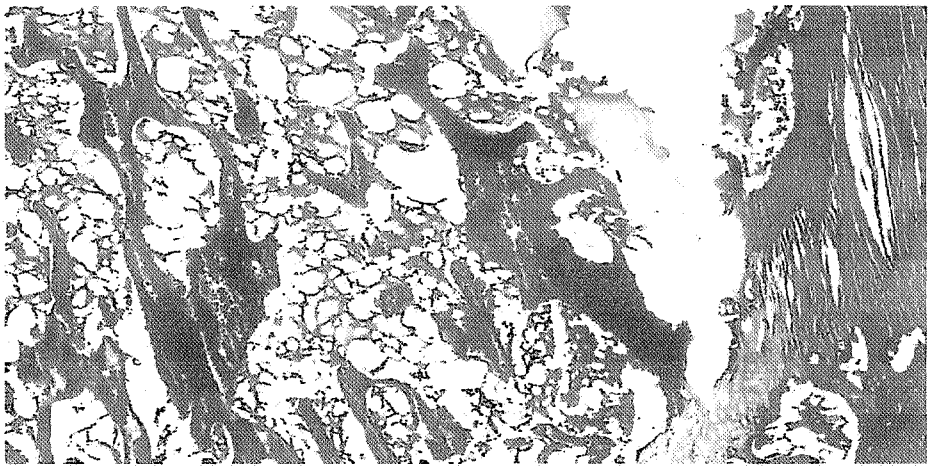

**Figure 3.7.B NPY dose 1, day one, x50, MT**

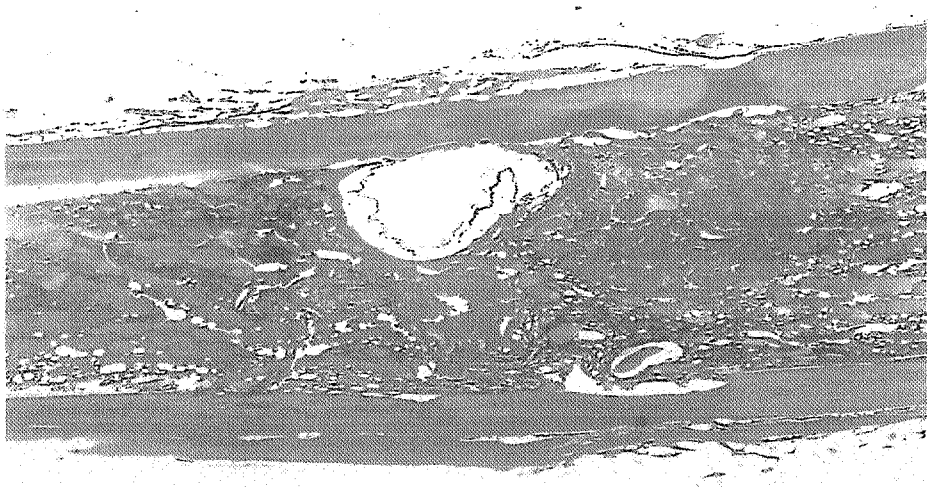

**Figure 3.7.C HA, 1st week, x25, HE**

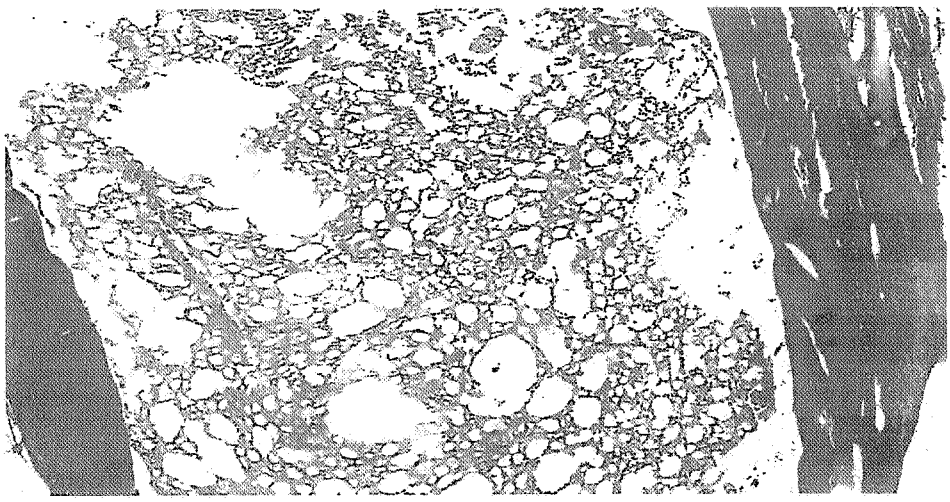

**Figure 3.7.D NPY dose1, 1st week, x50, MT**

**Figure 3.7.E NPY dose 2, 1st week, x50, HE**

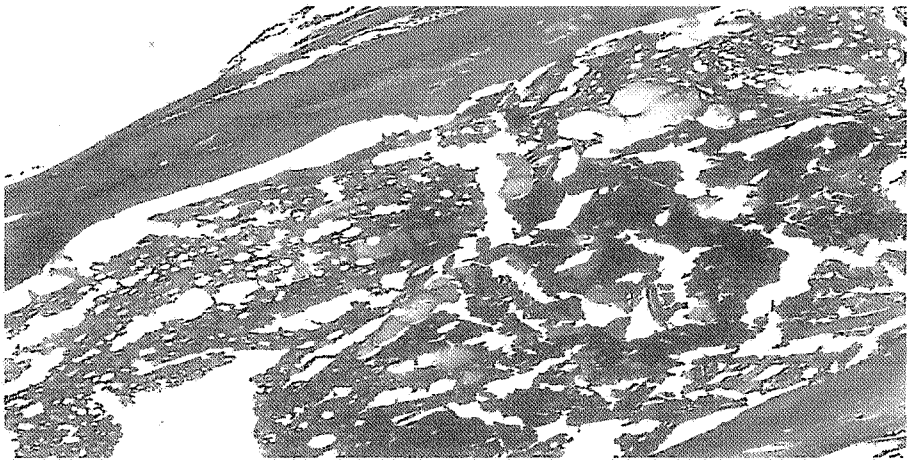

**Figure 3.7.F Inhibitor, 1st week, x50, MT**

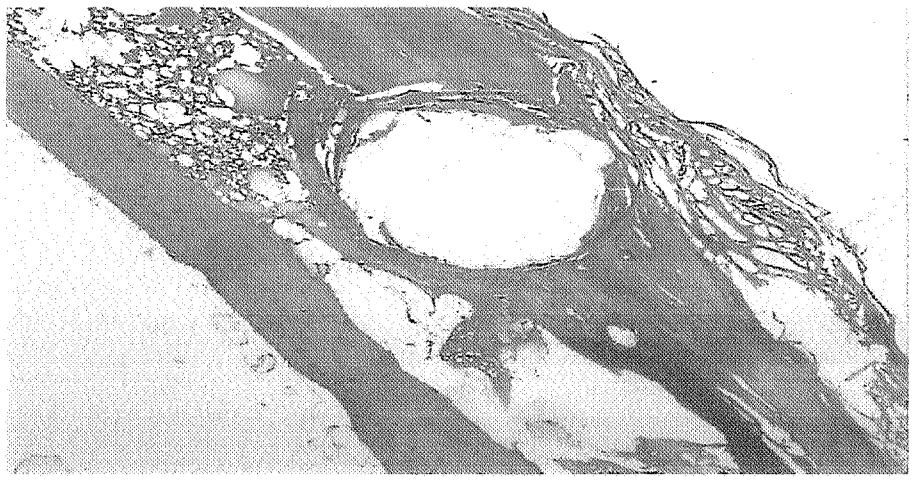

**Figure 3.7.G HA, 2nd week, x25, HE**

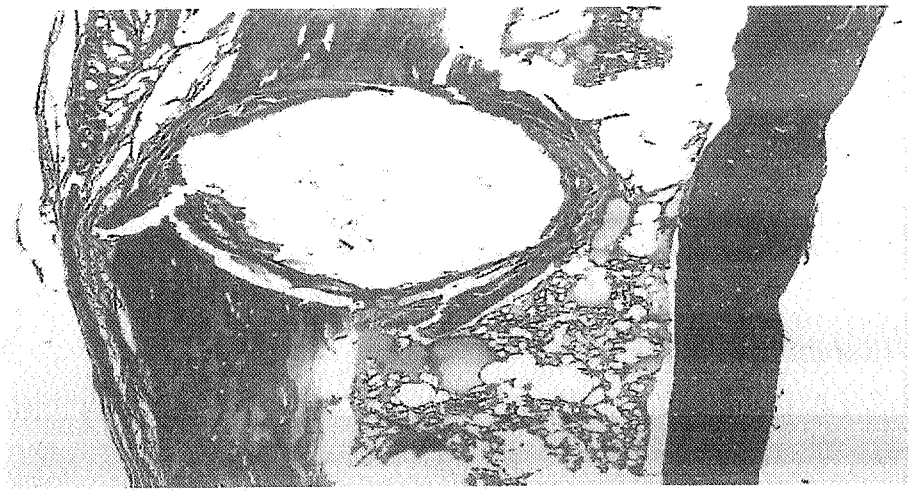

Figure 3.7.H HA, 2nd week, x25, MT

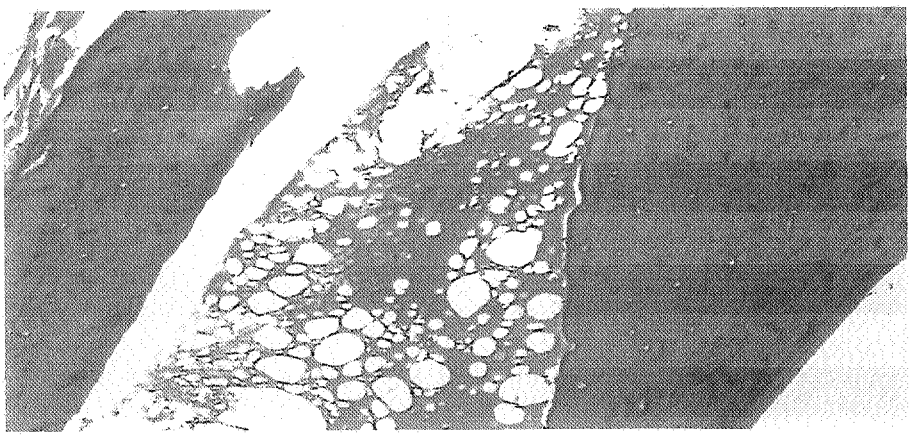

**Figure 3.1.I NPY dose2, 2nd week, x50, HE**

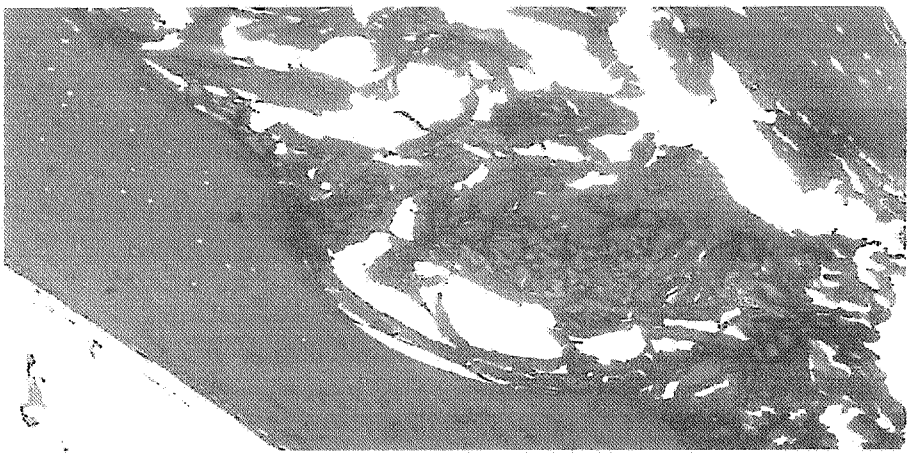

**Figure 3.7 J. NPY plus inhibitor, 2nd week, x50, MT**

### 3.9. Statistical Correlation of Data

It is observed that atomic content of cortex was correlated with density of cortex measured by QCT with **p**=0.00. In addition, atomic content of medulla was correlated with density of medulla measured by QCT with **p**=0.00, and densities of cortex and medulla both measured by QCT were correlated with **p**=.0.012. Statistical correlation of obtained data is presented at Table 3.7.

## Table 3.7 Statistical Correlation of Obtained Data

Correlations

| | | DEXA | ATOMICC | ATOMICM | QCTDENC | QCTDENM | TBP |
|---|---|---|---|---|---|---|---|
| DEXA | Pearson Correl | 1 | ,087 | -,005 | ,071 | -,087 | -,018 |
| | Sig. (1-tailed | . | ,329 | ,490 | ,360 | ,333 | ,476 |
| | N | 28 | 28 | 28 | 28 | 27 | 14 |
| ATOMIC | Pearson Correl | ,087 | 1 | ,225 | ,997* | ,399* | ,044 |
| | Sig. (1-tailed | ,329 | . | ,125 | ,000 | ,020 | ,441 |
| | N | 28 | 28 | 28 | 28 | 27 | 14 |
| ATOMIC | Pearson Correl | -,005 | ,225 | 1 | ,234 | ,942* | -,148 |
| | Sig. (1-tailed | ,490 | ,125 | . | ,116 | ,000 | ,307 |
| | N | 28 | 28 | 28 | 28 | 27 | 14 |
| QCTDEN | Pearson Correl | ,071 | ,997* | ,234 | 1 | ,432* | ,035 |
| | Sig. (1-tailed | ,360 | ,000 | ,116 | . | ,012 | ,453 |
| | N | 28 | 28 | 28 | 28 | 27 | 14 |
| QCTDEN | Pearson Correl | -,087 | ,399* | ,942* | ,432* | 1 | -,100 |
| | Sig. (1-tailed | ,333 | ,020 | ,000 | ,012 | . | ,367 |
| | N | 27 | 27 | 27 | 27 | 27 | 14 |
| TBP | Pearson Correl | -,018 | ,044 | -,148 | ,035 | -,100 | 1 |
| | Sig. (1-tailed | ,476 | ,441 | ,307 | ,453 | ,367 | . |
| | N | 14 | 14 | 14 | 14 | 14 | 14 |

**.Correlation is significant at the 0.01 level (1-tailed).

*.Correlation is significant at the 0.05 level (1-tailed).

### 3.10. Discussion:

Hyaluronic acid was used as a carrier system in this study. Although HA was observed to be biocompatible, it brought a limitation to the study. It was observed that HA's late degradation time limited the effecting dose of NPY. We concluded that experiments dependent on HA's degradation should be designed to meet follow up periods longer than two weeks. In addition, limited availability of rats in our current sources resulted in a restricted number of subject use in the experiments.

Another difficulty arose from the limited availability of number of literature parallel to our focus that would guide us in our procedures. We tried to adapt the amount of NPY to be administered from experimental procedures dealing soft tissue into bone. This study was based on such neuropeptide effect investigation studies (Rameshwar et al., 2002; Martinez et al. 1999). These studies indicated that minimum concentration of NPY should be $1x10^{-10}$ M at minimum to observe an easily detectable effect. We used $1x10^{-5}$ M and $1x10^{-6}$ M doses which were high enough to exert an effect if there existed any receptor of NPY and we were successful to obtain result.

Results of conventional radiography did not reveal any significant changes in bone mass. In a study which is of our type, this was an expected outcome. Because in two weeks period, we expected mild changes in bone mass and this change could not be easily recognized by conventional radiography due to technique's low ability to determine mild changes in bone. But conventional radiography was efficient to exclude fractured tibiae specimens from further analysis steps .

The results of DEXA analysis revealed interesting outcomes. From the first day to the second week of the study, there existed a consistent and significant increase in the means of bone density data of NPY plus inhibitor applied groups. We can infer from this result that NPY has reducing effect on bone mass by some intrinsic mechanisms; its inhibition causes significant increase in bone mass. Also, from the profile plot (**Figure 3.2.1**), we can easily observe that the means of bone density data in both NPY dose 1 ($1x10^{-5}$ M) and NPY dose 2 ($1X10^{-6}$M) applied groups almost remained constant throughout two weeks. From this data, we can deduce that existence of NPY alone did not cause any significant change in bone density. But according to *post hoc* analysis, which revealed significant correlation between control groups' (HA) and NPY dose 1 applied

groups' data ($p$=0.002), the effect of NPY was not same as the control group. NPY dose 1 applied groups had significantly lower bone density than control group. At this point, HA's activity captures our attention. Intramedullarly applied HA displayed a decrease in bone density form day one to week one and then a steep increase from week one to week two. By comparing HA applied tibiae with NPY plus inhibitor applied tibiae, we can deduce that HA applied tibiae experienced more osteoinductive effect than NPY plus inhibitor applied tibiae. Since NPY plus inhibitor were together applied with HA, their effect should be much close to HA's effect on tibiae alone. At this point, maybe it is logical to predict that NPY inhibitor that we used was unable to inhibit NPY dose 2 completely and NPY's and HA's effector mechanisms have reverse outputs on bone tissue (in intramedullary administration of both). According to our data, and with the knowledge of HA's osteoinductive effects (Huang, L. et al, 2002; Zanchetta, P. et al., 2003), NPY should have osteoclastic effect or inhibitory effects on bone formation. Also, NPY and HA should effect bone metabolism via intersecting pathways because when NPY dose 1 and NPY dose 2 together with HA were applied, the resulting bone density was lower than the HA's action by itself. NPY plus inhibitor and HA together displayed an intermediate action (in terms of bone mass) between NPY's and HA's application alone that can be a significance of

intersection. But suggesting a mechanism with data in our hand is beyond the scope of our study.

The results of cortex density measured by QCT implied that bone density of cortex of tibiae remained almost constant after week one through week two. NPY dose 1 applied group displayed a steep increase in bone density from day one to the week one (**Figure 3.2.2**). Almost a parallel increase were also observed in HA applied specimens from first day to second week, remaining constant from week one to the week two. Parallel with DEXA results, NPY plus inhibitor applied specimens also caused an increase in the bone density from day one to week one and remained almost constant from week one to week two.

Results of medullary density measured by QCT revealed a steep increase in bone density in NPY dose 1 applied tibiae's medulla from day one to week one; then a slight decrease from week one to week two. NPY dose 2 applied tibiae interestingly displayed a decrease in the first week and then remained almost constant through the second week (**Figure 3.2.3**). HA applied specimens almost followed the same pattern with a decrease in bone density from week one to week two. But NPY plus inhibitor applied species -consistent

with previous findings- followed a constant increase pattern from day one to the week two.

Results of atomic content of cortex of tibia measured by QCT revealed that NPY dose 1 displayed a step increase from day one to week one and remained almost constant from week one to week two. NPY dose 2 applied cortex of tibiae's effective atomic number remained almost constant throughout the study. NPY plus inhibitor applied group first displayed an increase from day one to week one and almost remained constant from week one to week two. Same pattern is also displayed by HA applied tibiae.

Results of atomic content of medulla of tibia measured by QCT revealed that NPY dose 1 applied group's medullary effective atomic number displayed an increase from day one to week one then a decrease from week one to week two. NPY dose 2 applied group displayed a decrease from day one to week one then remained constant through week two. NPY plus inhibitor applied group almost remained constant from day one to week one but then displayed an increase trend from week one to week two. HA applied group displayed an increase in the first week period than a decrease in the second week.

We did not expect any significant change in the first day data of three point bending (TPB) test. Stemming from this point, we did not evaluate rat tibiae on day one. Due to unavailability of rats in our facilities, we had to perform three point bending test with two rats for NPY dose 1, NPY dose 2, NPY plus inhibitor and one rat for HA group for (a) week one and (b) week two time points. From week one to week two, TPB results revealed that; NPY dose 1 applied groups gave rise to significant increase in bone strength, NPY dose 2 applied groups and NPY plus inhibitor applied groups brought about slight decrease in bone strength.

The results of histological analysis implied that HA as a drug carrier system was biocompatible with the repair tissue and neighboring tissue. HA seemed to exist inside the medullary cavity near the defect zone, seemed to withstand for some time, seemed to resorb gradually within three weeks and displaced itself with the new bone tissue and new medullary elements. Also, at the end of week two, histological findings displayed that new bone formation occurred in the intramedullary area og bone when NPY plus inhibitor was applied. This confirms the osteoinductive effect of HA (**Figure 3.7.J**).

Studies on hyaluronic acid (HA) and its structural relatives revealed that in optimal concentration and appropriate molecular weight, HA or structurally similar molecules have osteogenic and osteoinductive properties (Huang, L. et al, 2002; Zanchetta, P. et al., 2003) . In our study, HA stayed suspended in the medium longer than expected (3.7.G). Despite this prolonged existence of HA in the medium with its osteoinductive effects, NPY, which was co-existing with it, was able to cause a decrease or at least stability in bone mass throughout two weeks in the results except three point bending.

Three point bending test results did not reveal any significant change instead the increase in bone strength in second week in NPY dose 1 applied tibia compared to its analog in first week. The disadvantage of HA carrier system was its late degradation and for us, this produced a disadvantage for us from the time point aspect. We think that follow up time for three point bending test was inadequate to observe a change in bone strength.

Although the opposite have been reported by Ahmad T. et al, (2004), our experiment results also confirmed by histology observations can be interpreted as intramedullary acting NPY might

create changes in bone mass in favor of osteoclastic action. Another possibility is the inhibition of NPY in the intramedullary area might promote new bone formation around intramedullary area facing cortex. Considering the results obtained from this study, with intramedullary application procedure of NPY , it seems that NPY does not cause any significant change in the cortical area.

### 3.11. Conclusion:

With the data obtained from this study, we would like to make clinical experiments on fracture healing,bone regeneration and osteoporosis. Hopefully we would like to fulfill this data requirement for further clinical studies for wellbeing of humankind.

## REFERENCES


Ahmad T.,Morawski-Ugarph A,Li J.,Ljungar-Bileviciute I.,Finn A.,Östenson C.G.,Kreicbergs A. 2004, Bone and joint neuropathy in rats with type-2 diabetes Regulatory Peptides, article in press

Ahmed, M., Bjurholm A, Srinvasan GR, Theodorsson E, Kreicbergs A.,1994 Extraction of neuropeptides from joint tissue for quantitation by radioimmunoassay. A study in the rat. Peptides 15(2):317-22

Akin, S. and Kovscek, A.R., 2003, Computed tomography in petroleum engineering research. From: Mees, F., Swennen, R., Van Geet, M. and Jacobs, P. (eds). Applications of X-Ray computed tomography in the geosciences. Geological Society, London, Special Publications, 215, 23-28

Bjurholm A. , Kreicbergs A., Schultzberg M., 1989 Fixation and demineralization of bone tissue for immunohistochemical staining of neuropeptides. Calcif Tissue Int 45(4):227-31

Bjurholm A. 1991. Neuroendocrine peptides in bone. Int Orthop 15:325-329

Bjurholm, A., Kreicbergs, A.,Schultzberg, M. And Lerner, U.H.,1992 Journal of Bone and Mineral Research 7, 1011-1019;

Bjurholm, A., Kreicbergs ., Schultzberg M., 1989, Fixation and demineralization of bone tissue for immunohistochemical staining of neuropeptides. Calcif Tissue Int 45(4):227-31

Boyle et al., Nature 423, May 15 2003 page 349-55

Boyle et al., Osteoclast Differentiation and Activation Nature 423 May 15, 2003 page 337-341

Carter, D.R and Hayes, W.C., 1977, The compressive behavior of bone as a two phase porous structure Journal of Bone and Joint Surgery 59A:954-962

Chenu Chantal, 2002, Glutamatergic innervation in bone, Microscopy Research and Technique 58: 70-7

Cherruau M, Facchinetti P., Baroukh B, Saffar JL. Chemical sympathectomy impairs bone resorption in rats: a role for the sympathetic system on bone metabolism. Bone; 25(5): 545-51

Chine, C.,2002 Glutamic Innervation of Bone, Microscopy Research and Technique 58:70-76

Ducy, P. et al., 2000 Leptin Inhibits Bone Formation Through a Hypotalamic Relay: A central Control of Bone Mass Cell 100 197-207,

Favus, J. M ., editor, 1999 Primer on the metabolic bone diseases and disorders of mineral metabolism- an official publication of the American Society for Bone and Mineral Research, fourth edition, Lippincott Williams and Wilkins, pages 6-41, 134-137.

Freehafer A.A. and Mast W.A. 1965. Lower extremity fractures in patients with spinal cord injury. J Bone T Surg 47:683-694

Hardy A.G, Dickson J.W. 1963. Pathological ossification in traumatic paraplegia. J Bone T Surg 45: 76-87

Gillespie JA, 1963,The nature of bone changes associated with nerve injuries and disease. J Bone T Surg 36:464-473

Goldring S.R.,Goldring M.B. 1996 Cytokines and skeletal physiology, Clin. Orthop. 324:13-23

Harada and Rodan, Control of osteoblast function and regulation of bone mass, Nature 423,may 15 2003 page 349-55

Harada, S. and Gideon, A. R. Control of Osteoblast Function and Regulation of Bone Mass Nature 423 May 15, 2003 page 349-355

Lerner, 2002-Neuropeptidergic regulation of bone resorption and bone formation-J. Musculoskeletal Neuron Interaction 2(5):440-447

Hill E.L. and Elde R. 1991 Distribution of CGRP-, VIP-, D beta H-, SP- and NPY- immunoreactive nerves in the periosteum of the rat. Cell Tissue Res 264:469-480.

Holmgren and Jensen, 2001 Evolution of Vertebrate Neuropeptides - Evolution of the Nervous System, Brain Research Bulletin Vol55 No 6 PP 723-735

Hökfelt et al, Neuropeptides: Opportunities for a drug discovery 2003, Lancet Neurology ; 2:463-72

Huang L, Cheng YY, Koo PL, Lee KM, Qin L, Cheng JCY, Kumta SM, 2003. The effect of hyaluronan on osteoblast proliferation and differentiation in rat calvarial-derived cell cultures. J Biomed Mater Res 66a:880-884

Imai, S. and Matsusue, Y., 2002, Neuonal Regulation of Bone Metabolism and Anabolism: Calcitonin Gene-Related Peptide-, Substance P-, and Tyrosine Hydroxilase-Containing Nerves and the Bone, Microscopy Research and Technique, 58:61-69

Jamsa T, Jalovaara, P., Peng, Z.,Vaananen H.K. and Tuukkanen J., 1998, Comparison of three-point bending test and peripheral quantitative computed tomography analysis in the evaluation of the strength of mouse femur and tibia, Bone, Vol. 23, No.2 August 1998: 155-161

Kaplan et al., Formand Function of Bone Orthopedic Basic Science Columbus, OH, American Academy of Orthopedic Sciences

Karsenty, Gerard The complexities of skeletal biology Nature 423 May 15,2003 page 317-321

Kontinnen Y et al.,1996 Neuropeptide and the puzzle of bone remodeling Acta Orthop Scand. 67:1737-1740

Lerner U.H., 2002, Neuropeptidergic regulation of bone resorpption and bone formation J.Musculoskeletal Neuron Interact ; 2 (5): 440-447

Lerner, U.H,1996 Kinins and neuropeptides In: Principles of Bone Biology: San Diego: Academic Press Page s 581-586

Lindbald , B.E. 1994 et al. Vasoconstrictive action of NPY in bone Acta Orthop Scand 65(6): 629-634

Lodish, Berk, Zipursy, Baltimore, Darnell Molecular Cell Biology, 5th Edition page G-12 glossary,

Lundberg, J.M., et al. 1996 Pharmacology of cotransmissions in the autonomic nervous system: Integrative aspects on amines, neuropeptides, adenosine triphosphate and nitric oxide. Pharmacology Review 48,113-178

Lundberg, P. and Lerner U. H. 2002, Expression and Regulatory Role of Receptors for Vasoactive Intestinal Peptide in Bone Cells, Mic. Res. and Tech. 58:98-103

Lundberg, P., Lundgen, I., Mukohyama, H., Lehenkari, P.P., Horton, M.A. and Lerner, U.H. (2001) Endocrinology 142, 339-347:

Rahman, S., Dobson, P. R., Bunning, R. A., Russel R.G., and Brown, B. L. (1992) Regulatory Peptides, 37, 111-121;

Rameshwar, P. et al. Vasoactive intestinal peptide (VIP) inhibits the proliferation of bone marrow progenitors through the VPAC1 receptors Experimental Hematology 30 (2002) 1001-1009

Reddy, G.K., Stehno-Bittel L., Shigeharu H., Enwemeka, C.S., 2001, The biomechanical integrity of bone in experimental diabetes, Diabetes Research and Clinical Practice 54:1-8

Rice, J.C., Cowin, S.C., and Bowman, J.A. (1988). On the dependency of the elasticity and strength of cancellous bone on apparent density. Journal of Biomechanics 21:155-168

Serre CM et al., 1999 Evidence for a dense and intimate innervation of bone tissue, including glutamate containing fibers Bone 25 : 623-629

Serre CM et al.,2000 Neuroctemy in growing rat induces a bone loss associated with a reduction of nerve profiles J. Bone Miner. Res. 14(Suppl:1): Page 242

Shier, D. et al.,1996 Hoe's Human Anatomy and Physiology, Eighth Edition, pages 160-272

Spencer G.J., Hitchcock, I.S. and Genever, P. G. (2004) Emerging Neuroskeletal Signalling Pathways: A Review, FEBS Letters, 559, 6-12

Spencer, G.J.,Hitchcock I.S, Genever G.G.,2004, Emerging neuroskeletalsignalling pathways: a review, FEBS Letters, 559, 6-12

Takeda, S. et al. Leptin Regulates Bone Formation via Sympathetic Nervous System. Cell 111, 305-317 (2002)

Thorsell A. and Heilig M. ,2002, Diverse functions of NPY revealed using genetically modified animals. Neuropeptides 36 (2-3),182-193

Togari A., 2002, Adrenergic regulation of bone metabolism: Possible involvement of sympathetic innervation of osteoblastic and osteoclastic cells. Microscopy Research and Technique 58:77-84

Togari, A., Arai, M., Mizutani, S., Koshihara, Y. and Nagatsu, T. (1997) Neuroscience Letters 233, 125-128;

Turner, C. H. And Burr, D. B.,1993, Basic biomechanical measurements of bone: A tutorial, Bone, 14, 595-608